Quantum Control of Radical-Pair Dynamics beyond Time-Local Optimization

Farhan T. Chowdhury, Matt C.J. Denton, Daniel C. Bonser, and Daniel R. Kattnig[*]

Department of Physics and Astronomy, University of Exeter, Stocker Road, Exeter EX4 4QL, United Kingdom

We realize arbitrary-wave-form-based control of spin-selective recombination reactions of radical pairs in the low-magnetic-field regime. To this end, we extend the gradient-ascent pulse engineering (GRAPE) paradigm to allow for optimizing reaction yields. This overcomes drawbacks of previously suggested time-local optimization approaches for the reaction control of radical pairs, which were limited to high biasing fields. We demonstrate how efficient time-global optimization of the recombination yields can be realized by gradient-based methods augmented by time blocking, sparse sampling of the yield, and evaluation of the central single time-step propagators and their Fréchet derivatives using iterated Trotter-Suzuki splittings. Results are shown for both a toy model, previously used to demonstrate coherent control of radical-pair reactions in the simpler high-field scenario and, furthermore, for a realistic exciplex-forming donor-acceptor system comprising 16 nuclear spins. This raises prospects for the spin control of actual radical-pair systems in ambient magnetic fields, by suppressing or boosting radical reaction yields using purpose-specific radio-frequency wave forms, paving the way for reaction-yield-dependent quantum magnetometry and potentially applications of quantum control to biochemical radical-pair reactions. We demonstrate the latter aspect for two radical pairs implicated in quantum biology.

I. INTRODUCTION

The rapidly evolving field of optimal quantum control (OQC) seeks to manipulate phenomena at the quantum scale by devising and implementing perturbations, typically in the form of electromagnetic pulses, to steer a given quantum system to a desired target. Fueled by demonstrable successes in nuclear magnetic resonance (NMR) pulse engineering [1–3] and the control of ultrafast excited-state reactions by laser fields [4], pioneering developments in "coherent control" were first conceived in chemistry. Today, OQC has developed into a mature discipline that is central to modern quantum technologies associated with the second quantum revolution [5], with numerous applications across quantum information processing and quantum metrology [1]. Following on from an earlier proposal for controlling the dynamics of radical-pair reactions through modulating the exchange interaction via an optically switchable bridging group [6,7], a recent suggestion extends coherent control to radical-pair reactions mediated through radio-frequency (rf) magnetic fields [8], thereby putting a renewed spotlight on the quantum control of

spin-chemical reactions. In the present work, we go on to demonstrate the implementation of a gradient-ascent pulse engineering- (GRAPE) inspired approach, made computationally feasible via novel algorithmic modifications, toward realizing open-loop control of singlet recombination yields for radical-pair dynamics in weak magnetic fields.

Reactions involving the recombination of radical-pair intermediates are well known to depend on spin degrees of freedom and their intrinsic quantum dynamics. Specifically, the electronic singlet and triplet states associated with the unpaired electrons for each radical can undergo coherent interconversion as a consequence of symmetry-breaking interactions; in particular, the hyperfine interactions with surrounding magnetic nuclei. Quite recently, quantum beats reflecting the coherent singlet-triplet interconversion in radical pairs have been directly revealed through pump-push spectroscopy [9]. In the case of singlet and triplet states exhibiting differential chemical reactivity, which is usually the case since radical-pair recombination preserves spin multiplicity in the absence of strong spin-orbit coupling, the spin dynamics are reflected in the reaction yields realized via the singlet and triplet channels. By coupling to magnetic fields via the Zeeman interaction, radical pairs furthermore acquire sensitivity to static and oscillatory applied magnetic fields. The former is central to various magnetic field effects (MFEs) associated with radical-pair reactions, while the latter are pertinent to the prospect of radical-pair reaction control through

---

rf magnetic fields. Studies of effects of oscillatory magnetic fields on radical-pair reactions have been realized for chemical model systems and play a discriminatory role in identifying magnetosensitive radical-pair reactions in spin-biological systems [10,11].

While a majority of model studies on oscillatory magnetic field effects have applied monochromatic rf magnetic fields in the presence of a strong biasing field [12], often referred to as reaction-yield-detected magnetic resonance (RYDMR), some studies have been realized in a weak static field; in particular, for exciplex-forming systems [13–17]. In such systems, consisting of an electronically excited donor-acceptor complex characterized by partial charge transfer and photoemissivity [18], the radical pair is in equilibrium with or can populate an exciplex state. In this way, radical-pair dynamics become accessible and/or measurable via the exciplex emission, i.e., the recombination yield is proportional to the fluorescence emission under steady-state conditions [19]. Radical-pair-mediated mechanisms, or variations thereof [20], are also hypothesized to underpin a compass sense in various animals, including migratory songbirds [21]. In this case, the magnetosensitive radical pair is thought to originate from a photoinduced electron transfer reaction in the flavoprotein cryptochrome. Even though the exact nature of the underlying radical pair has remained unclear, the fact that this compass sense is interruptible by weak monochromatic [22] or broadband rf [23] magnetic fields strongly supports an underlying spin-mediated mechanism. These observations support the prospect of controlling chemical reactions involving radical pairs, possibly in the near future, in the spin-biological context, and the challenging low-field regime, provided that an efficient approach to pulse engineering can be developed, as we set out to do in our present work.

Recent work [8,24] has suggested the control of radical-pair reactions based on model calculations for a prototypical spin system. They focus on the traditional RYDMR scenario, for which the applied electromagnetic field is in resonance with the electronic Zeeman splitting produced by a strong static field. This perturbs the singlet-triplet interconversion of the radical pair and thus affects the yield of geminate recombination. Their control approach, building upon the theoretical approach developed by Sugawara [25], propagates the spin-density operator, whereby at every moment the control amplitude is chosen such that an optimization criterion is bound to not decrease. Since the algorithm optimizes the controls in a time-local fashion, it is dubbed as *local optimization*. By construction, the employed algorithm allows optimization of the trajectory of an observable commuting with the time-independent dynamics generator, i.e., the drift Hamiltonian, or alternatively, an arbitrary observable at *one* chosen moment in time (via back propagation). While the combined population of the singlet (S) and one of the triplet states (T_0)

is hence controllable over time in the high-field limit, the more relevant singlet population falls into the second category. Through our present work, we overcome ostensible drawbacks of the time-local optimization approach by permitting time-global optimization that simultaneously optimizes the controls for all times and by focusing on the singlet recombination yield, i.e., the actual experimental observable (rather than S and T_0 populations over time or the singlet probability at a moment in time). We achieve this through using piecewise constant control amplitudes and gradient information, by building upon GRAPE [26]. To realize quantum control of radical-pair dynamics in a weak static magnetic field, these developments are critical.

Our approach, even in the framework of controls derived for prototypical models not explicitly considering weakly coupled nuclear spins and spin-relaxation processes, promises robustness in applications to more realistic system descriptions. This opens avenues for an OQC-based model-tomography approach to distinguish between candidate radical pairs in systems where magnetosensitivity is phenomenologically observable but the underpinning mechanisms remain opaque. Enabling the discriminatory shaping of magnetosensitive responses could prove to be particularly fruitful for pinning down key facilitating mechanisms, with applications ranging from magnetoreception [21] to organic spintronic materials [27], or for enhancing sensitivity for the imaging of magnetic nanostructures [28]. Further potential avenues for exploration are magnetic field measurements, e.g., via delayed fluorescence-based organic light-emitting diodes with large magnetoelectroluminescence [29], or for medical and biological applications [30], where selected pathways could potentially be controlled, possibly to endpoints not reachable via static magnetic field exposure alone.

We deviate from traditional GRAPE by optimizing reaction yields (rather than a fidelity measure defined at a given moment in time), accounting for asymmetric radical-pair recombination, which gives rise to nonunitary propagators, using exact gradients rather than approximate ones, and, following de Fouquieres *et al.* [31], by using curvature information of the loss function (rather than steepest decent or ascent). To overcome a major objection to GRAPE-based reaction control of radical pairs, namely, high computational demands, as also voiced by Masuzawa *et al.* [8], we suggest a number of practical optimizations, such as a block-optimization scheme and sparse sampling of the reaction yield to improve the efficiency of the approach while retaining adequate control fidelity. With these improvements, realistically large radical-pair systems can be yield controlled in weak magnetic fields. We demonstrate the success of the approach for a large spin system in an exciplex-forming complex and further provide examples motivated by quantum biology.

II. THEORY

A. Radical-pair spin dynamics

We consider a system comprising radicals $A^{\bullet-}$ and $B^{\bullet+}$ subject to singlet-triplet interconversion, undergoing spin-selective recombination reactions as per Fig. 1. The corresponding spin dynamics are described in terms of the time-dependent spin-density matrix $\hat{\rho}(t)$ by

$$\frac{d\hat{\rho}(t)}{dt} = -i[\hat{H}(t), \hat{\rho}(t)] - \{\hat{K}, \hat{\rho}(t)\}, \qquad (1)$$

with $\hat{H}(t)$ denoting the spin Hamiltonian and

$$\hat{K} = \frac{k_S}{2}\hat{P}_S + \frac{k_T}{2}\hat{P}_T \qquad (2)$$

accounting for radical-pair recombination. Here, k_S and k_T denote the reaction-rate constants in the singlet and triplet state, respectively, and $\hat{P}_S$ and $\hat{P}_T$ are the projection operators onto the singlet and triplet states. We introduce an effective Hamiltonian given by

$$\hat{A}(t) = \hat{H}(t) - i\hat{K}, \qquad (3)$$

allowing us to reformulate Eq. (1) as

$$\begin{aligned}\frac{\partial \hat{\rho}(t)}{\partial t} &= -i[\![\hat{A}(t), \hat{\rho}(t)]\!] \\ &= -i(\hat{A}(t)\hat{\rho}(t) - \hat{\rho}(t)\hat{A}(t)^\dagger),\end{aligned} \qquad (4)$$

where $[\![A, B]\!] = AB - (AB)^\dagger = AB - BA^\dagger \ \forall \ B = B^\dagger$. The formal solution to Eq. (4) is given by

$$\hat{\rho}(t_n) = \hat{U}(t_n, 0)\hat{\rho}(0)\hat{U}^\dagger(t_n, 0), \qquad (5)$$

where the time-evolution operator in terms of $\hat{A}(t)$ is

$$\hat{U}(t, 0) = \mathcal{T}\exp\left[-i\int_0^t \hat{A}(\tau)d\tau\right]. \qquad (6)$$

Here, $\mathcal{T}$ denotes the time-ordering operator, which reorders products of time-dependent operators such that their time arguments decrease going from left to right.

The singlet-channel recombination yield is given by

$$Y_S = k_S \int_0^\infty p_S(t)dt, \qquad (7)$$

where $p_S(t) = Tr[\hat{P}_S\hat{\rho}(t)]$ is the survived-singlet probability of the radical pair. Note that Eq. (4) is of truncated
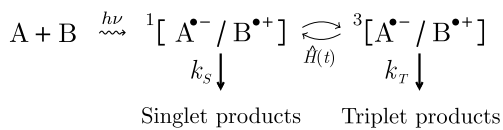
Lindblad form (by introducing shelving states, an equivalent formulation in traditional Lindblad form is also possible [32]). Thus, the essentially open quantum system description of radical-pair spin dynamics in the presence of spin-selective recombination [Eq. (1)] can be treated in terms of the dynamics of a closed system, albeit with a non-Hermitian dynamics generator, nonunitary evolution operators, and nonconserved trace.

Here, we consider radical pairs for which the static part of the Hamiltonian, $\hat{H}_0$, is of the form

$$\hat{H}_0 = \hat{H}_A + \hat{H}_B + \hat{H}_{AB}, \qquad (8)$$

where $\hat{H}_i, i \in \{A, B\}$ is local to radical i and comprises the Zeeman interaction with the static magnetic field and isotropic hyperfine couplings with surrounding nuclear spins. $\hat{H}_{AB}$ accounts for inter-radical couplings in the form of the exchange interaction. Specifically, each radical is described in terms of corresponding nuclear and electron-spin angular-momentum operators $\hat{\mathbf{I}}_{ik}$ and $\hat{\mathbf{S}}_i$ by

$$\hat{H}_i = \omega_i\hat{S}_{iz} + \sum_{k=1}^{n_i} a_{ik}\,\hat{\mathbf{I}}_{ik}\cdot\hat{\mathbf{S}}_i \qquad (9)$$

and

$$\hat{H}_{AB} = -j_{ex}\left(2\hat{\mathbf{S}}_A\cdot\hat{\mathbf{S}}_B + \frac{1}{2}\right), \qquad (10)$$

where $\omega_i = -\gamma_i B$, with γ_i denoting the gyromagnetic ratio of the electron in radical i and B the applied magnetic field, a_{ik} is the isotropic hyperfine coupling constant between electron spin i and the kth nuclear spin (out of total n_i), and the exchange-coupling constant is denoted by j_{ex}. The initial density operator is assumed as

$$\hat{\rho}(0) = \frac{1}{Z_1 Z_2}\hat{P}_S, \qquad (11)$$

where $Z_i = \prod_{k=1}^{n_i}(2I_{ik} + 1)$ is the total number of nuclear spin states in radical i and

$$\hat{P}_S = \frac{1}{4} - \hat{\mathbf{S}}_1\cdot\hat{\mathbf{S}}_2, \qquad (12)$$

the singlet projection operator. In the context of our exploration of quantum biological systems, we also consider directional magnetic field effects of systems with anisotropic hyperfine interactions. In this case, $\hat{H}_i$ is of the form

$$\hat{H}_i = \omega_i\mathbf{n}(\vartheta, \varphi)\cdot\hat{\mathbf{S}}_i + \sum_{k=1}^{n_i}\hat{\mathbf{I}}_{ik}\cdot\mathbf{A}_{ik}\cdot\hat{\mathbf{S}}_i, \qquad (13)$$

where $\mathbf{n}(\vartheta, \varphi)$ is a unit vector with polar angle ϑ and azimuth φ defining the magnetic field direction and the $\mathbf{A}_{ik}$s are the hyperfine tensors.

$$A + B \xrightarrow{h\nu} {}^1[\,A^{\bullet-}/B^{\bullet+}\,] \underset{\hat{H}(t)}{\rightleftarrows} {}^3[A^{\bullet-}/B^{\bullet+}\,]$$

$$k_S\downarrow \qquad\qquad k_T\downarrow$$

Singlet products   Triplet products

FIG. 1. The reaction scheme.

B. Gradient-based coherent control

Here, we outline pertinent features and extensions of our GRAPE-inspired approach. Borrowing its basic setup from GRAPE, our approach entails discretizing controls into time slices that are improved in a concurrent-update scheme, i.e., involving controls for all time points (thus "time-global"), with each update determined only by information from the previous iteration, so that they can be evaluated at each point independently. Specifically, in GRAPE, the gradient of the fidelity (usually defined at a predefined final time) with respect to all control variables is calculated (or rather approximated) in each iteration and a step is made in the variable space in the direction of steepest ascent (or descent). For quantum systems controllable via convex optimization, first-order gradient information can sufficiently guarantee that the global maximum at the top of the control landscape can be located from any given direction, with the extremes of a given control landscape corresponding to either perfect control or no control [33].

Without loss of generality, we can describe a given quantum system undergoing spin dynamics under coherent control with

$$\hat{H}(t) = \hat{H}_0 + \sum_{l=1}^{M} u_l(t)\hat{V}_l, \qquad (14)$$

where $\hat{H}_0$ is the drift Hamiltonian describing the time-independent part of the system, i.e., the intrinsic radical-pair dynamics in the static bias field, as introduced above, $u_l(t)$ are the control amplitudes and $\hat{V}_l$ is the set of control Hamiltonians that couple the controls to the system, e.g., via the Zeeman interaction. We control parameters of only the coherent evolution of the open-system dynamics of the radical pair undergoing spin-selective recombination reactions. In principle, the recombination could also be directly controlled. However, direct control of recombination is less amenable to experimental manipulation and therefore is not pursued here.

The goal of OQC is to optimize some control objective functional $G[\{u_l(t)\}]$, with a control target subject to physical constraints and other criteria. For our purposes, we focus on minimizing or maximizing the singlet recombination yield of the radical pair, i.e., $G = Y_S$, as outlined in Fig. 2. However, the approach is easily generalized to focus on other reaction outcomes, e.g., accumulated nuclear polarization. Significant prior work has been concentrated on optimizing G subject to the assumption that the values taken by the controls over time may be parametrized by piecewise constant control amplitudes in the time domain [34]. This paradigm, which is central to GRAPE as the first widely applied quantum control algorithm [26], is well aligned with the practical aspect of controlling radical pairs, as standard arbitrary-wave-form-generator- (AWG) based control schemes represent pulse

inputs as piecewise constant functions. We thus discretize the time axis, $t_0 = 0 < t_1 < t_2 < \cdots < t_N = t_{max}$ and we set

$$\hat{H}(t) \approx \hat{H}_0 + \sum_{l=1}^{M} \sum_{n=1}^{N} u_{l,n}\chi_n(t)\hat{V}_l, \qquad (15)$$

with constants $u_{l,n}$ and the indicator function $\chi_n(t)$ defined such that

$$\chi_n(t) = \begin{cases} 1 & \text{for } t_{n-1} \leq t < t_n \\ 0 & \text{otherwise} \end{cases}.$$

The corresponding propagators $\hat{U}(t_n, 0)$ are discretized on the temporal grid such that

$$\hat{U}(t_n, 0) = \mathcal{T}\prod_{i=1}^{n} \hat{U}_i = \hat{U}_n \cdots \hat{U}_1, \qquad (16)$$

where

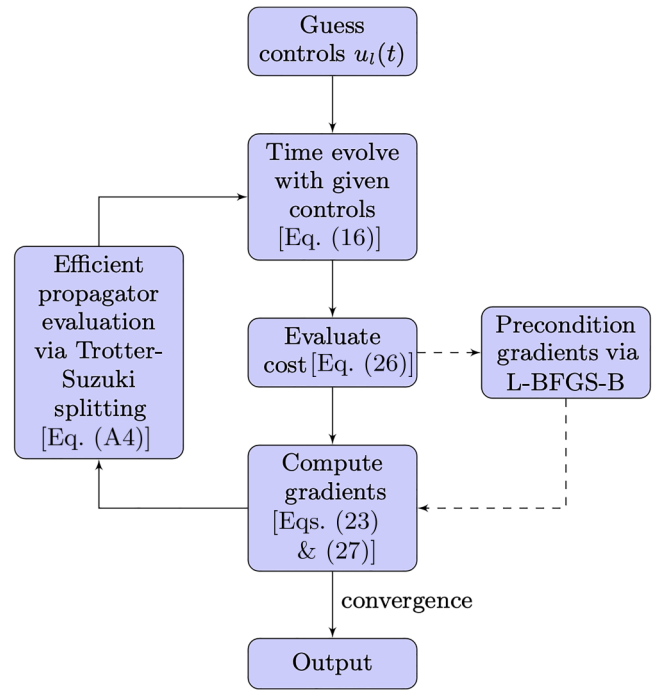$$\hat{U}_i = e^{-i\hat{A}_i\Delta t_i}, \qquad (17)$$

FIG. 2. A simplified flowchart for optimizing radical-pair reaction yields. Initially, the control variables are guessed, and the system is time evolved. The fidelity is then computed in terms of an objective function and we obtain an output where convergence is achieved. Otherwise, the gradient with respect to control variables is computed and utilized, together with iteratively accumulated curvature information, to update the controls, using which the system is again time evolved and the process repeats.

with $\Delta t_i = t_i - t_{i-1}$ and $\hat{A}_i = \hat{A}(t_{i-1})$. The gradients of G depend on the propagator derivatives, evaluated as

$$\frac{\partial \hat{U}_i}{\partial u_{l,j}} = \delta_{i,j} L_{i,l} = \delta_{i,j} L(i\hat{A}_i \Delta t_i, i\hat{V}_l \Delta t_i), \qquad (18)$$

where $L(X, E)$ is the Fréchet derivative of the matrix exponent defined, for every E, by

$$e^{(X+E)} - e^X = L(X, E) + o(\|E\|). \qquad (19)$$

More explicitly, we have [35]

$$L(X, E) = \int_0^1 e^{X(1-s)} E e^{Xs} ds$$

$$= \sum_{n=1}^{\infty} \frac{1}{n!} \sum_{j=1}^{n} X^{j-1} E X^{n-j}, \qquad (20)$$

which also allows us to demonstrate that

$$\frac{\partial \hat{U}_i^\dagger}{\partial u_{l,j}} = \delta_{i,j} L(+i\hat{A}_i^\dagger \Delta t_i; +i\hat{V}_l \Delta t_i)$$

$$= \delta_{i,j} L^\dagger(-i\hat{A}_i \Delta t_i; -i\hat{V}_l \Delta t_i)$$

$$= \delta_{i,j} L_{i,l}^\dagger. \qquad (21)$$

Combining the above equations, the gradient of the survived-singlet probability,

$$p_S(t_n) = Tr[\hat{P}_S \hat{U}(t_n, 0) \hat{\rho}(0) \hat{U}^\dagger(t_n, 0)], \qquad (22)$$

for $k \leq n$, is thus

$$\frac{\partial p_S}{\partial u_{l,k}} = -i Tr(\hat{P}_S \hat{U}_+ [\![\hat{W}_{k,l}, \hat{U}_- \hat{\rho}_0 \hat{U}_-^\dagger]\!] \hat{U}_+^\dagger)$$

$$= -i Tr(\hat{U}_+^\dagger \hat{P}_S \hat{U}_+ [\![\hat{W}_{k,l}, \hat{U}_- \hat{\rho}_0 \hat{U}_-^\dagger]\!])$$

$$= 2\Im[Tr(\hat{U}_+^\dagger \hat{P}_S \hat{U}_+ \hat{W}_{k,l} \hat{U}_- \hat{\rho}_0 \hat{U}_-^\dagger)]$$

$$= 2\Im[Tr(\hat{P}_S \hat{U}_+ \hat{W}_{k,l} \hat{U}_- \hat{\rho}_0 \hat{U}^\dagger)], \qquad (23)$$

where $\hat{W}_{i,l} = i\hat{U}_i^{-1} L_{i,l}$ and

$$\hat{U}_+ = \mathcal{T} \prod_{m=k}^{n} \hat{U}_m, \qquad (24)$$

$$\hat{U}_- = \mathcal{T} \prod_{m=1}^{k-1} \hat{U}_m. \qquad (25)$$

For $k > n$, the gradient obviously vanishes. In the original formulation of GRAPE, a first-order approximation of $L_{k,l}$ has been used [26], which is obtained with $\hat{W}_{i,l} = \hat{V}_l$. For

our approach, we use the full Fréchet derivative. Finally, this allows us to approximate the singlet yield by

$$Y_S = k_S \int_0^\infty p_S(t) dt$$

$$\approx k_S \sum_{n=0}^{N} w_n p_S(t_n), \qquad (26)$$

with w_n denoting suitably chosen quadrature weights. The gradient of the singlet yield is then obtained as

$$\frac{\partial Y_S}{\partial u_{l,k}} \approx k_S \sum_{n=k}^{N} w_n \frac{\partial p_S}{\partial u_{l,k}}. \qquad (27)$$

III. RESULTS

The control of radical-pair dynamics using time-global optimization methods is expected to be computationally costly, which is why Masuzawa *et al.* [8] had dismissed GRAPE in favor of time-local optimization in their earlier attempt at realizing radical-pair reaction control. The computational demand is particularly large if, as we do here (and unlike Refs. [8,24]), the goal is to optimize yields, which are time-integral quantities [cf. Eq. (7)], unlike the typical fidelity measures in quantum control applications pertaining to the implementation of a state transfer or a unitary operation for a fixed time t_{max}. Nevertheless, we succeed in being able to demonstrate the feasibility of a time-global approach for radical-pair systems of realistic complexity through leveraging various algorithmic modifications.

A. Algorithmic efficiency improvements

We require the computation of N single-time-step propagators alongside their Fréchet derivatives with respect to L control Hamiltonians and scores of repeated matrix multiplications to evaluate the time-dependent singlet probabilities and associated gradients, which sum to the recombination yield and its associated gradients. In the Appendix, we evaluate the number of required matrix multiplications (scaling with N^2), leading to the key insight that for the considered scenario and typical Ns and problem sizes, the cost of gradient or expectation-value evaluation will exceed that of evaluating the elementary propagators and their derivatives (scaling with N). To allow for efficiently optimizing the reaction yield of radical pairs, we thus suggest the adaptation of the gradient-based optimization procedure as illustrated in Fig. 3.

First, we argue that the optimization can be realized in practice in terms of B disjoint blocks of N/B time steps each (time blocking). Second, we suggest that a sparsely sampled, i.e., crude, approximation of the reaction yield based on $N/(BS)$ samples per block, i.e., sampling
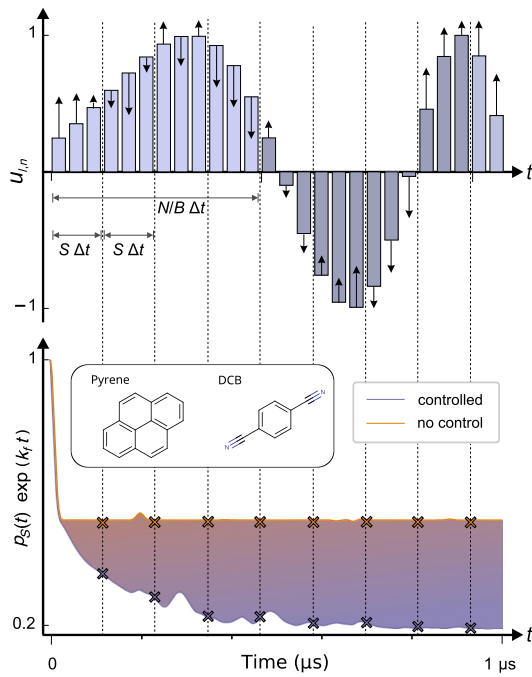
FIG. 3. A schematic illustration of the time-blocking and sparse-sampling approach used to reduce the computational expense of gradient-based optimization of the radical-pair recombination yield. The control amplitudes $u_{l,n}$ are simultaneously updated, whereby B disjoint blocks of $\frac{N}{B}$ time steps each are considered in succession, with the initial state taken to be that of the system subject to the preceding optimized controls. A sparsely sampled approximation of the reaction yields based on $\frac{N}{BS}$ samples per block suffices to effectively optimize the reaction yield, in particular for larger spin systems for which the singlet probability is barely oscillatory. The bottom panel illustrates the unperturbed (orange solid line) and minimized (blue) singlet probability for pyrene–para-dicyanobenzene (Py-DCB), an 18-spin exciplex system in a static biasing field of 1 mT. The rf control field of 0.1-mT amplitude comprised 1024 control pulses of 1-ns width, the amplitude of which has been optimized such that the singlet yield approximately calculated from 256 samples of the singlet probability has been minimized assuming a recombination rate of $k = 1\ \mu s^{-1}$. The Py-DCB system is discussed in more detail in the text.

every S-th time-step, is sufficient to adequately optimize the reaction yield. Here, B and S are integers that divide N and N/B, respectively. While this approach formally does not yield the optimum of the yield as defined in Eq. (7), henceforth referred to as the complete optimum, we argue that for suitably chosen B and S, yields optimized through sparsely sampled time blocking, realized at a fraction of the computational effort, are sufficiently close to the true optimum. Third, to efficiently calculate the exponential propagators and the associated Fréchet derivatives, we use a scaling and squaring approach in combination with a Trotter-Suzuki splitting of the elementary propagator, as detailed in the Appendix. Lastly,

to accelerate the optimization, we utilize L-BFGS-B, a limited memory variant of the Broyden-Fletcher-Goldfarb-Shanno algorithm, which preconditions gradients with curvature information in lieu of steepest descent [31].

B. Protocol applied to a prototypical spin system

We consider the minimization of the singlet recombination yield for a generalization of the prototypical radical pair studied earlier in the work by Masuzawa *et al.* [8], where coherent control of a fidelity measure, rather than the reaction yield, has been achieved in the simpler high-field scenario using time-local optimization. Specifically, we assume a radical pair comprising seven spin-$\frac{1}{2}$ particles, coupled through isotropic hyperfine (0.2, 0.5, and 1 mT and 0.2 and 0.3 mT for the two radicals, respectively) and exchange interactions ($j_{ex}/(2\pi) = 1$ MHz), undergoing spin-selective recombination in the singlet state with rate constant $k_b = 1\ \mu s^{-1}$ or spin-independent escape with rate constant $k_f = 1\ \mu s^{-1}$, such that $k_S = k_b + k_f$ and $k_T = k_f$. Given the high computational demands of completely optimizing the seven-spin system, we have additionally studied the five-spin system resulting from the seven-spin system by retaining the three largest hyperfine coupling constants. Unlike Masuzawa *et al.* [8,24], we seek to directly minimize the singlet recombination yield

$$Y_b = \frac{k_b}{k_b + k_f} Y_S \qquad (28)$$

through a piecewise constant control field applied perpendicular to a static biasing field, i.e., $L = 1$ and $V \equiv V_1 = \omega_1(\hat{S}_{1,x} + \hat{S}_{2,X})$, where ω_1 is the maximal Rabi frequency of the control field; the control amplitudes are subject to $|u_{1,n}| \equiv |u_n| \leq 1$. We chose a discretization time step of 1 ns and controlled the first 5 μs ($N = 5000$) after initialization of the spin system in the singlet electronic state (thus accounting for more than 99.3% of radical decay; the final yields still evaluated in the $t \to \infty \sim t_{max}$ limit with $t_{max} = 14$ μs). In Fig. 4, we illustrate exemplary time-dependent singlet probabilities, controlled and unperturbed, associated with this scenario for the biasing field intensities $B_0 = 0.5$ mT and 10 mT.

Efficient evaluation of single-time-step propagators, and their Fréchet derivatives, has been made possible via iterated Trotter-Suzuki splittings, and time blocking and sparse sampling of reaction yields, as introduced above. In view of Fig. 5 and comparable data sets for other biasing fields provided in the Supplemental Material [36] (cf. Fig. S4), it is apparent that excellent control results can be achieved for all N/B block sizes exceeding 500. Neither $B = 1$ nor $N = B$ are strict necessities for practical control of the reaction outcome: substantially smaller blocks yield comparable optimization results at a fractional cost. On the other hand, block sizes of 50 and 100 are unsatisfactory, indicating that a time-local optimization is insufficient
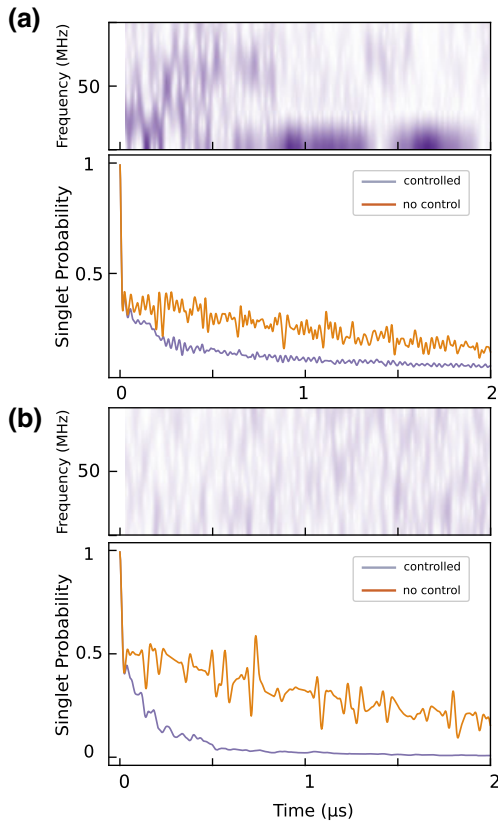
(a)

(b)

FIG. 4. (a),(b) The controlled recombination dynamics of a seven-spin radical-pair system under (a) 0.5-mT and (b) 10-mT static biasing fields. The plots depict the survived-singlet probability [cf. Eq. (23)] with (blue) and without (orange) coherent control, scaled to remove the spin-independent decay, i.e., $p_S(t) \exp(k_f t)$. The recombination yield has been minimized over $N = 5000$ time steps split into $B = 2$ blocks of 2500 time steps each, sampled sparsely at $S = 5$ and $S = 10$ for (a) and (b), respectively. The accompanying spectrograms display the control-field magnitudes, computed via discrete Fourier transforms of 64 points, overlapped by 60 points, and windowed using a Tukey function with a shape parameter of 0.25. Using a control amplitude of 0.25 mT, the singlet recombination yield could be reduced to 0.156 (from 0.269 without control) and 0.097 (from 0.346) for the two biasing fields.

to yield optimal control results in the low- to intermediate-field region. For these inadequate block sizes, results of the utilized L-BFGS-B optimization is, furthermore, strongly dependent on the initial condition. Note that intermediate block sizes N/B are occasionally preferred over larger optimization blocks, as the latter are less prone to get stuck in local minima, such that the overall optimization outcome can be superior. This is seen in, e.g., Fig. S4 of the Supplemental Material [36] for a biasing field of 1 mT, for which the best result of six replicated optimizations with $B = 2$ and $B = 5$ happens to surpass those with $B = 1$. Note furthermore that the optimization results for smaller biasing fields, e.g., 0.5 mT, are more sensitive to the sampling interval, S, than for 10 mT. This is not surprising in

view of the more varied singlet probability as a function of time observed for the lower field. This is encouraging insofar as more complex spin systems with diverse hyperfine interactions are expected to be less oscillatory. In any case, it appears that sampling intervals S of 25 and less are adequate here.

For the seven-spin system, we found it impractical to realize a complete set of optimizations for $S = 1$ and $B = 1$, i.e., complete unblocked optimization, as optimization runs initiated from random configurations required more than a week to finish on the hardware utilized. However, a complete optimization starting from the best blocked optimization finished swiftly for the used tolerances, without yielding a significant additional improvement. Furthermore, a single complete optimization yielded results comparable to those of the good blocked and sparsely sampled optimizations. For the smaller five-spin system, it is apparent that the sparsely sampled blocked optimizations converge smoothly to the completely sampled optimum and that, again, $B > 1$ and $S > 1$ allow excellent practical optimization outcomes relative to this (expensive) limit. For these and further optimization results achieved for the five- and seven-spin systems in weak magnetic fields, including the geomagnetic field, see Fig. 5(b) and the Supplemental Material [36] (cf. Figs. S1 and S2).

With the approach established, we set out to explore the prospects offered by controlling radical-pair reaction yields in the weak to intermediate field case. In Fig. 6(a), we illustrate the results of minimizing the singlet recombination yield as a function of the applied static magnetic field relative to the unperturbed scenario. These results have been realized using five blocks of 1000 time steps of 1 ns and sampling the recombination yield from every 25th time point. The maximal control amplitude was 0.25 mT. The plotted whiskers indicate 75-percentiles from seven optimizations, starting from random initial controls. Evidently, the recombination yield can be markedly reduced for all applied fields, the lowest yield realizable being 0.0966, realized for a biasing field of 9 mT. This amounts to a reduction by more than a factor of 3.5 compared to the uncontrolled yield at the same field (0.346). Generally, it is remarkable that the yields controlled for minimal recombination are all markedly lower than the minimal recombination yield of 0.252 realizable by applying a static magnetic field of 0.2 mT, i.e., the field matching the dip in the singlet yield attributed to the low-field effect.

We have further analyzed the dependence of the optimization outcome on the strength of the control field. In Fig. 6(b), we show Y_b as a function of the maximal control amplitude for the case of a static biasing field of 10 mT and 50 μT, again realized by optimizing five blocks of 1000 time steps, sampling every 25th. Appreciable minimization for $B_0 = 10$ mT requires control amplitudes of 0.1 mT; controls with field strength below approximately 50 μT do not elicit appreciable effects. This finding is
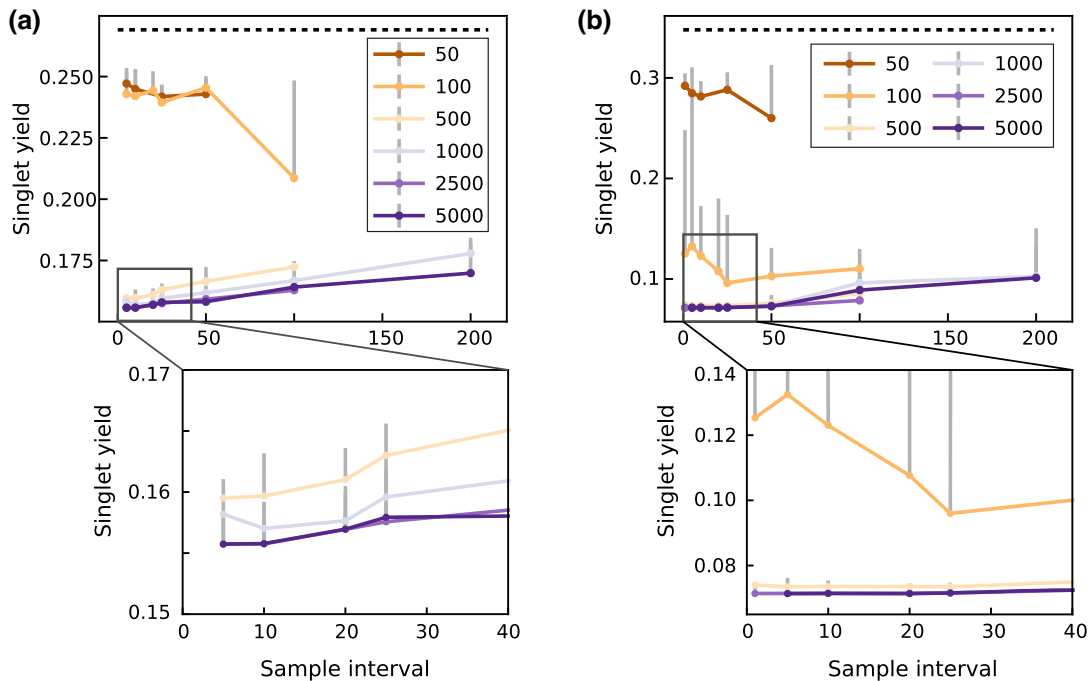
FIG. 5. (a),(b) For the seven- and five-spin model systems and a maximal control-field amplitude of 0.25 mT, with biasing fields of (a) 0.5 and (b) 10 mT, we show the singlet recombination yield as a function of S for yield minimizations using B blocks of N/B steps each, the latter values being reported in the keys ($N = 5000$). The plots present the best minimization result from six independent replications with randomly chosen initial control amplitudes (chosen from a normal random distribution truncated at ± 1); with dots indicating the 75-percentile range. The best optimization results allow a reduction of the singlet recombination yield from 0.269 to 0.156 and from 0.348 to 0.071 for (a) and (b), respectively.

in line with the well-studied effects of rf magnetic fields on radical pairs. In this scenario too, a resonant perturbation can only appreciably impact the spin evolution during the radical-pair lifetime, τ, if $-\gamma B_1/(2\pi)\tau \gtrsim 1$, i.e., if the lifetime is sufficiently large to permit at least one Larmor precession in the field associated with the perturbation. As here $k_f^{-1} = 1$ μs and $k_b^{-1} = 1$ μs, we can expect effects for B_1 exceeding 36–72 μT to become effective, which is in tentative agreement with the observed B_1 dependence. On the other hand, driving fields larger than 0.1 mT allow very significant reductions of the recombination yield. It is interesting to note that for controlling reaction outcomes in the geomagnetic field ($B_0 = 50$ μT), slightly larger control fields exceeding 0.12 mT are required.

Above, we have assumed that controls are applied with a time resolution of $\Delta t = 1$ ns. While AWGs are available with sufficient sample rates and analog bandwidths (e.g., 50 Gsamples/s at 15 GHz bandwidth) and the delivery of broadband magnetic fields at the required intensity has been realized (e.g., for high-field electron-nuclear-double-resonance (ENDOR) spectroscopy [37]), the question of the minimal bandwidth to control radical-pair reactions is a pertinent one. To this end, we have studied the dependence of the control result on the "speed limit" enforced on the control signal. Specifically, we have stipulated that the controls must obey $|u_n - u_{n-1}| < \dot{u}_{\max}\Delta t$. For $B_0 = 1$

mT, in Fig. 6(c) we summarize the dependence of the singlet yield on this speed limit. We find that transition times of $\dot{u}_{\max}^{-1} \lesssim 8$ ns are required to elicit significant control; fast controls only deliver marginal additional gains. The minimal speed limit corresponds to a bandwidth of approximately $\dot{u}_{\max}/2 = 63$ MHz, which is of the order of, but smaller than, the magnitude of the spread of energy eigenvalues of the radical pair (93 MHz).

C. Protocol applied to a realistic exciplex-forming radical pair

We now present results for coherently controlling the symmetric recombination of a large spin system consisting of 18 spins. We consider the Py-DCB exciplex-forming donor-acceptor systems in a solvent of moderate polarity [16,38,39]. The magnetosensitive delayed fluorescence emission of this system has been widely studied. To make this large-scale simulation tractable, we limit ourselves to the scenario of homogeneous decay, i.e., $k_S = k_T = k$, and neglect inter-radical interactions. While this may appear crude at first glance, models typical of this have seen considerable success in the interpretation of experimental data [40]. The approximations are adequate since for the majority of its lifetime, the radical pair is in fact diffusively well separated and the moderate reaction asymmetry of the
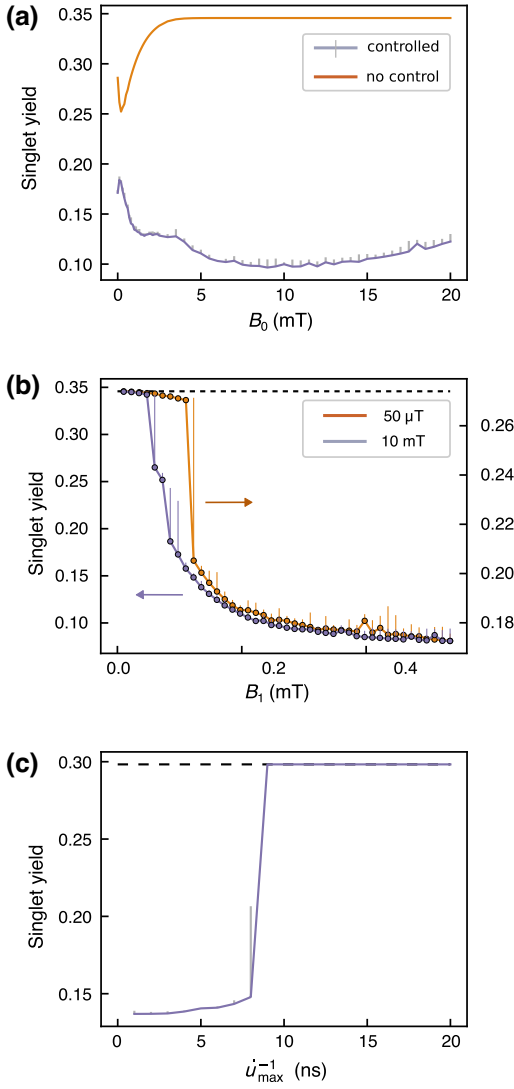
FIG. 6. The dependence of the optimization outcome on the field strength of the biasing field and the driving field, and the control speed for the seven-spin model system. (a) We consider a 0.25 mT control field and show yield minimization against increasing B_0 (blue) in comparison to the uncontrolled reference (orange). (b) We show yield minimization against an increasing control-field amplitude, B_1, for a biasing field of $B_0 = 10$ mT and 50 µT. (c) We show the dependence of the singlet recombination yield at $B_0 = 1$ mT on the speed limit $\dot{u}_{max}^{-1}$. For all optimizations, $N = 5000$, $B = 5$, and $S = 25$.

real system (resulting from different electron-transfer-rate constants in the singlet and triplet state; the latter to the locally excited triplet state) has all but a small effect on the magnetic field sensitivity. Thus, in this limit, the singlet probability can be expressed as

$$p_S(t) = e^{-kt}\left(\frac{1}{4} + \sum_{\alpha\beta\in\{x,y,z\}} R_{\alpha,\beta}^{(1)}(t)R_{\alpha\beta}^{(2)}(t)\right), \quad (29)$$

where

$$R_{\alpha\beta}^{(i)}(t) = \frac{1}{Z_i}\mathrm{Tr}\left[\hat{S}_{i\alpha}(0)\hat{S}_{i\beta}(t)\right]$$
$$= \frac{1}{Z_i}\mathrm{Tr}\left[\hat{S}_{i\alpha}\hat{U}^\dagger(t,0)\hat{S}_{i\beta}\hat{U}(t,0)\right] \quad (30)$$

are the electron-spin correlation tensors for each spin in radical i, which are defined or calculable in the Hilbert space of the individual radicals. Here, $\hat{U}$ accounts for the coherent evolution only, i.e., $\hat{A}(T) = \hat{H}(T)$ [cf. Eq. (6)]. Thus, control of the radical-pair reaction yield can be realized by separately calculating the gradients for each of the spin correlation tensors of two recombining radicals and assembling the gradient of the reaction yield using the chain rule. Again, we follow the ideas of blocking the time axis and sparse sampling to increase the efficiency. In addition to the Trotter-Suzuki splitting discussed above, we use the fact that the Hamiltonian is only a function of the total nuclear spin associated with groups of completely equivalent spins, which permits an efficient calculation in the "coupled representation" [41]. In Fig. 7, we show the minimization of the Py-DCB singlet recombination yield for $k^{-1} = 200$ ns, a control amplitude of 0.2 mT, and a static biasing field of 10 mT. The control has been extended to the first 1024 time steps of 1 ns each. Varying the block and sample sizes again confirms practically sufficient fidelity from noncomplete optimization, as is demonstrated in Fig. 7(b) (also see Fig. S3 in the Supplemental Material [36]). In our view, exciplex-systems of the type discussed here would be ideally suited to realize first proof-of-principle experimental realizations of OQC of radical-pair reaction yields [9,16,18,38,39] by building on the time-resolved MFE measurements and studies of rf effects that have already been realized.

D. Applications to quantum biology

Many observations of biochemical magnetosensitivity appear to be attributed to radical-pair intermediates in complex biological environments [21,30]. We anticipate that the control of radical-pair reactions will develop into a versatile applied field, particularly in the spin-biological context. Static and oscillatory magnetic fields can and have been used to perturb such systems, but these naive controls are neither selective for specific pathways nor can reaction yields be changed drastically. But our OQC approach promises distinguishability of reaction pathways involving different radical pairs and enlarged effect sizes in weak biasing fields, such as the geomagnetic field. We demonstrate this potential here in terms of two selected examples with a quantum biological underpinning.

The flavin semiquinone (FADH$^\bullet$)-superoxide (O$_2^{\bullet-}$) radical pair has been suggested to underpin various magnetic field sensitive biochemical processes, such as MFEs on
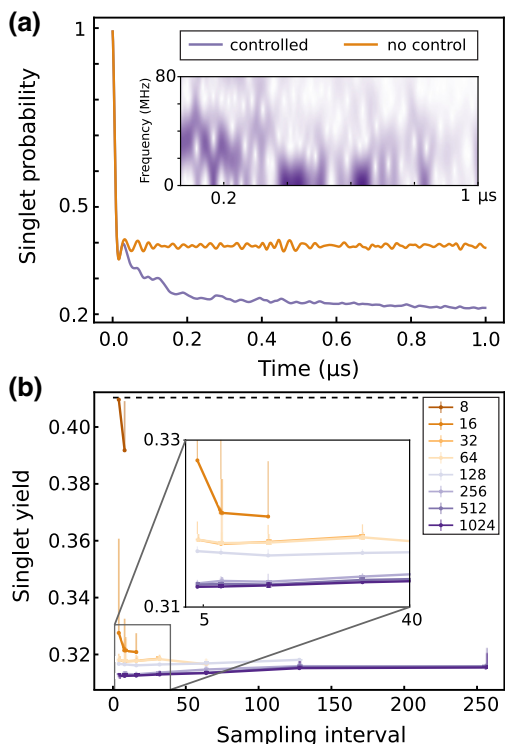
FIG. 7.   Recombination-yield minimization of the 18-spin Py-DCB system in a bias field of 1 mT. (a) The singlet probability, scaled to remove the spin-independent decay due to radical recombination, i.e., $p_S(t) \exp(kt)$, with and without control. The control amplitudes have been optimized using 32 samples and 1024 time steps of 1 ns; a spectrogram of the control-field magnitude is shown as an inset. (b) The final yield as realized using L-BFGS-B complemented gradient optimization for increasing sampling intervals and various block sizes, N/B, as indicated in the legend.

neurogenesis [42] and cellular energetics [43]. Being of so-called reference-probe type, this radical pair is renowned for its sensitivity to weak magnetic fields [44] but questions concerning its potentially fast spin relaxation remain [45]. We consider the limit of slow spin relaxation, conventionally referred to as the FADH$^\bullet$/Z$^\bullet$ model. Here, Z$^\bullet$ denotes a radical that is devoid of hyperfine interactions and slowly relaxing, i.e., an idealization of O$_2^{\bullet-}$, as it might be approached in the real system through immobilization. In Fig. 8, we show the ability of our approach to maximize the recombination yield of the triplet-born radical pair. This model, with parameters taken from Ref. [46], exhibits a large low-field effect in response to a static magnetic field (orange line). Controlling the recombination (blue line) allows us to boost the recombination efficiency, realizing recombination yields that are not achievable by the application of static magnetic fields of any strength. In the biological context, this would lead to a decrease of superoxide release from flavin reoxidation reactions, thereby reducing the concentration of free superoxide. Superoxide

is a central reactive oxygen species that assumes important roles as a signaling molecule, thus linking radical-pair reactions to central biological control pathways [47]. Since magnetosensitivity in a physiological setting is currently not well understood beyond circumstantial evidence, the latter is a more distant aim, albeit an auspicious one, because it could allow the targeting of specific redox pathways in isolation for various applications; e.g., wound healing [48] or the suppression of the adverse effects of hypomagnetic field [42,49] exposure for space travel. Other future applications might be the control of chemical reactions for synthetic purposes, e.g., in the context of flavin photocatalysis [50].

In sensory biology, a certain consensus has been reached attributing an inclination compass in birds and various other species to the proposed radical-pair mechanism involving the flavoenzyme cryptochrome [21]. However, the identity of the actual magnetosensitive radical pair is still subject to debate. *In vitro* experiments on cryptochromes have demonstrated the magnetosensitivity of a photoinduced radical pair comprising the flavin anion radical (FAD$^{\bullet-}$) and a surface-exposed tryptophan cation radical (W$^{\bullet+}$), implicating FAD$^{\bullet-}$/W$^{\bullet+}$ as the sensory species [51]. However, magnetoreception appears to also be possible in the dark, suggesting the potential involvement of a reoxidation pathway, once more implicating the flavin semiquinone-superoxide radical pair (FADH$^\bullet$-O$_2^{\bullet-}$) in magnetoreception. Furthermore, various alternative radical pairs have been suggested in theoretical studies demonstrating superior magnetic field sensitivity, e.g., for ascorbyl and Z$^\bullet$ containing radical pairs [44]. Given the multitude of suggestions and hypothesis, the distinguishability of various radical pairs in biology is a timely question. This question cannot be resolved by direct spectroscopic means, as the radical pair is a transient intermediate in a complex biological environment in a living organism. Here, we demonstrate that OQC could, at least in principle, provide the sought-after insights.

We have considered models of the FAD$^{\bullet-}$/W$^{\bullet+}$ and FADH$^\bullet$/Z$^\bullet$ radical pairs, including the anisotropic hyperfine interactions of the dominant nuclear spins in a relative orientation as found in a cryptochrome (parameters taken from [52]). The recombination yield of this system depends on the orientation of the geomagnetic field relative to the protein frame. The difference of the maximal and minimal yield, realized for field directions $\mathbf{n}_{max}$ and $\mathbf{n}_{min}$, i.e., $\Delta_S = Y_S(\mathbf{n}_{max}) - Y_S(\mathbf{n}_{min})$ is considered a measure of the sensitivity of the radical-pair-based compass. In Fig. 9, we demonstrate the ability of OQC to control, i.e., maximize or minimize, this performance parameter for the two radical pairs considered. The control fields have been applied parallel to the geomagnetic field. The excitation profiles have been optimized for one radical pair and its performance subsequently evaluated in both. We find that OQC can significantly alter, enhance, or
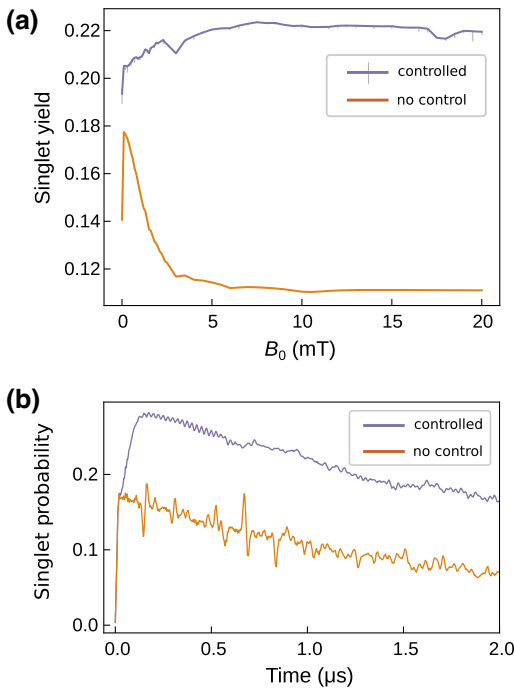
FIG. 8. (a) The controlled and unperturbed singlet recombination yield of a flavin semiquinone-superoxide radical pair, abstracted as FADH$^\bullet$/Z$^\bullet$, initialized in the triplet state, as a function of the applied static biasing field. The radical pair has been assumed to undergo a spin-independent decay or escape reaction with rate constant $k_f = 1 \ \mu s^{-1}$ and spin-selective recombination in the singlet state with rate constant $k_b = 1 \ \mu s^{-1}$. The first 5 μs after radical-pair generation have been controlled using a stepwise constant control field with 1-ns time resolution and a maximal amplitude 0.25 mT, applied perpendicular to the static magnetic field. The control has been optimized using the L-BFGS-B algorithm applied to five blocks of 1 μs, sampling the yield every 25 ns. The optimizations have been repeated 5–6 times, starting from random initial controls; with the error bars indicating the 75-percentile range of best results (the variability between runs is noticeably small compared to the change in recombination yield produced through control). (b) The time dependence of the singlet probability of the radical pair in a 4-mT biasing field in the absence and presence of the optimized control field, scaled to remove the spin-independent decay, i.e., $p_S(t)\exp(k_f t)$. The associated singlet recombination yields amount to 0.218 and 0.115 with and without controls, respectively.

attenuate Δ_S for both radical pairs. Importantly, sequences optimized for one pair turn out to only have a minor effect on the spin dynamics of the other. Thus, the control fields are selective, permitting us to distinguish the two models insofar as they induce a large effect on the singlet recombination-yield contrast in the targeted pair and a negligible effect in the competitor. In particular, the controls derived for FAD$^{\bullet-}$/W$^{\bullet+}$ appear as an apt tool to realize such an experiment, because the contrast Δ_S is strongly altered, the system specificity is high,

the time of radical-pair generation is controllable using pulsed photoexcitation, and the parameters pertaining to FAD$^{\bullet-}$/W$^{\bullet+}$ are best known, as they are available from *in vitro* experiments and derivable from crystal structures and computational-chemistry methods. Clearly, here we limit ourselves to only demonstrating principal feasibility; more detailed models will have to be studied before instigating actual experiments.

The robustness of our derived control pulses to small changes is central for future applications. While control engineering generally aims to capture the intricacies of the control target as closely as possible, in practice our knowledge of the actual spin-Hamiltonian parameters [53] might be limited or the available computational resources might restrict the optimization to a simplified spin system comprising only the strongest hyperfine-coupled nuclear spins. In this context, controls derived from simplified systems, in particular those not accounting for weakly coupled nuclear spins or spin-relaxation processes, are crucial. As evidenced in the Supplemental Material [36], controls derived using our approach are indeed robust when applied to simulations accounting for the relevant inhomogeneous hyperfine interactions via the Schulten-Wolynes framework [54] (cf. Fig. S5 in the Supplemental Material [36]). The controls are also found to be robust against noise in the form of random field fluctuations, which induce decoherence and spin relaxation (cf. Fig. S6 in the Supplemental Material [36]). In particular, we find that the controls derived for idealized systems retain their unique property of permitting recombination yields that cannot be realized using a static magnetic field of any flux density even in the presence of spin relaxation and unresolved hyperfine interactions.

IV. DISCUSSION

In electronic and nuclear spins of organic radical pairs, coherence lifetimes on the order of 100 ns to microseconds are typical, even in complex biological environments [55], opening a window of opportunity to realize control by applying time-dependent magnetic fields to manipulate reaction outcomes. Yet, the approach is still in its infancy. Experimental approaches have been limited to perturbing radical-pair spin systems by rf magnetic fields [17,23]. While positioned far from optimal control, these experiments are crucial, as they demonstrate the principal possibility of influencing radical-pair dynamics by rf magnetic fields in weak magnetic fields. Examples of rf magnetic field effects are, furthermore, well established for biological radical pairs *in vivo* [17], such as those supposedly underpinning the avian compass sense. The latter are particularly noteworthy, because surprisingly weak rf magnetic fields have been found to interrupt magnetoreception, suggesting an exquisitely sensitive underlying system with a remarkable coherence time.
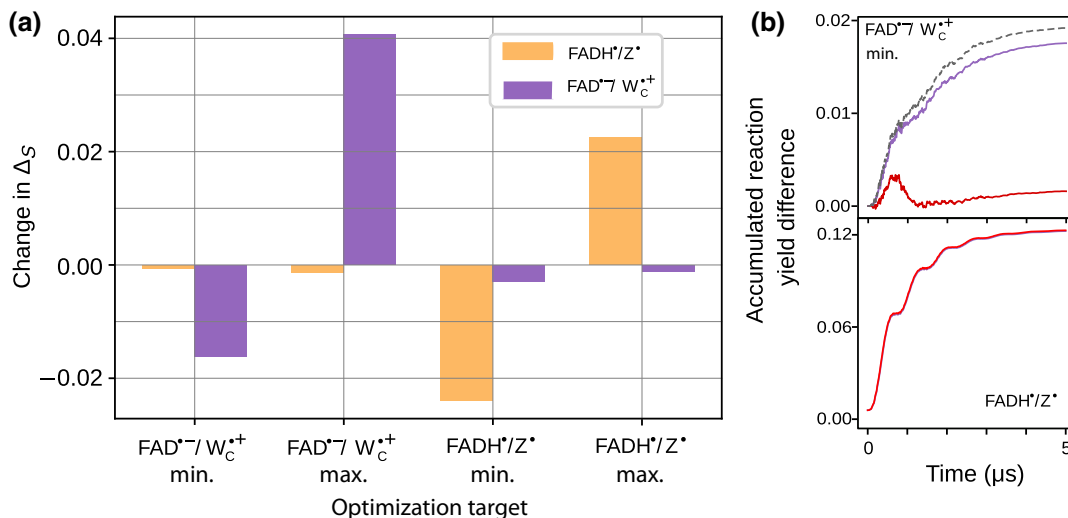
FIG. 9. (a) The change in the singlet yield contrast Δ_S for $FAD^{\bullet-}/W^{\bullet+}$ and $FADH^\bullet/Z^\bullet$ radical pairs subject to controls optimized to maximize or minimize the singlet recombination-yield contrast Δ_S in the geomagnetic field for one of the pairs (as indicated in the axis labels). The geomagnetic field has been assumed as $50\,\mu T$ and the radical-pair lifetime $1\,\mu s$, i.e., $k_S = k_T = 1\,\mu s^{-1}$. The control has been applied parallel to the static field with an amplitude of $12.5\,\mu T$. The first $5\,\mu s$ after radical-pair generation in the singlet state have been controlled with a time step of $1\,ns$. Yields have been calculated by integrating to $t_{max} = 14\,\mu s$. The optimization has been realized through 40 steps of steepest descent or ascent. The unperturbed singlet yield contrasts are $\Delta_S = 0.017$ and 0.13 for $FAD^{\bullet-}/W^{\bullet+}$ and $FADH^\bullet/Z^\bullet$, respectively. (b) The accumulated reaction yield differences for each, $k_S \int_0^t p_S(n_{max}, t) - p_S(n_{min}, t)\,dt$, i.e., the accumulated yield difference up to time t as a function of time for the $FAD^{\bullet-}/W^{\bullet+}$ (top panel) and $FADH^\bullet/Z^\bullet$ (bottom panel) radical pairs. The red lines for each radical pair correspond to the case of the radical-pair dynamics being perturbed by the OQC-derived perturbation targeting the minimization of Δ_S for $FAD^{\bullet-}/W^{\bullet+}$. The $FADH^\bullet/Z^\bullet$ pair is practically unresponsive to this perturbation (bottom panel), while the directional sensitivity of $FAD^{\bullet-}/W^{\bullet+}$ is mostly attenuated. For $FAD^{\bullet-}/W^{\bullet+}$, the gray line applies to the scenario of applying a harmonic perturbation with frequency $1.4\,MHz$, demonstrating that designed perturbations are significantly more disruptive than unspecific perturbations.

Optimal quantum control protocols could be used to drive chemical and spin-biological systems in a controlled and selective way, whereby reaction outcomes not attainable by static magnetic field perturbations alone become accessible. For quantum information processing in near-term quantum hardware, among the many hurdles faced in counteracting environment-induced decoherence is the need to realize precise timing of quantum gate operations [56,57] on nanosecond time scales. To avoid this bottleneck, precise or adaptive [4,58,59] quantum control protocols may be harnessed to change the frequency of an applied control field dynamically throughout its pulse duration. But this is often hard to realize in practice, since formulating the appropriate optimal quantum control protocols is often highly nontrivial. In nature, radical pairs seem to avoid the effects of decoherence to retain exceptionally long coherence times, resulting in exquisite and unparalleled magnetometric sensitivity even in extremely noisy biological settings. Thus, optimal quantum control protocols, formulated with the primary aim of reproducing this sensitivity in spin-chemical reactions in solution, could also inform methods for similarly realizing artificial or biological molecular [17,60] qubits highly sensitive to applied magnetic fields. This could translate to further applications [56,61–63] in both quantum metrology and quantum information processing. In particular, potential engineering principles derived from gleaning deeper physical insights gained from artificially driving radical-pair reactions could conceivably inspire a new generation of quantum enhanced sensing technologies for magnetometry boasting heightened sensitivity and robustness against noise [7,61,63–67]. But to realize this goal, and future applications of optimal quantum control in a potentially biological context, efficient approaches to control design are vital.

The control of radical-pair reactions is distinct from the majority of OQC approaches in the sense that as the optimization target is not defined at a particular instant of time but is encoded in the time evolution from radical-pair creation to its eventual decay, $t \in [0, \infty)$, i.e., the reaction yield. Here, we have generalized the GRAPE paradigm of using piecewise constant control amplitudes to realize reaction yield control. The suggested algorithm aims to overcome the limitations of a previous approach by targeting actual reaction yields (rather than continuously updating the control to optimize a fidelity function involving observables that commute with the Hamiltonian or the singlet probability at one instance of time)

and permitting control in weak magnetic fields. A time-global update scheme of control parameters (as opposed to the time-local approach from Ref. [8,24,25]), central to GRAPE, has here been found essential to realize the latter efficiently. The computational cost of controlling radical-pair reaction yields by time-global optimization techniques such as GRAPE has been viewed as prohibitive [8]. And, indeed, significant computational costs are associated with the evaluation of the numerous single-time-step propagators and their Fréchet derivatives, and, for the optimization of reaction yields in particular, the calculation of the time-integral recombination yield and its gradient through iterated matrix multiplications involving the former. We have introduced a block-optimization scheme and sparse sampling of the reaction yield to improve the efficiency of this step while retaining adequate control fidelity. To facilitate the efficient evaluation of propagators and their derivatives, we have utilized an iterated Trotter-Suzuki splitting. We further leverage curvature information of the loss function in lieu of standard steepest-descent or steepest-ascent approaches to reduce the number of optimization steps required, as previously suggested [31].

The additional algorithmic modifications that we incorporate into our GRAPE-inspired approach are vital for addressing the high computational costs, which have impeded earlier attempts to realize GRAPE-based reaction control of radical-pair dynamics. We note that while sparse sampling of the reaction yield provides a useful low-cost proxy for the actual reaction yield, we have found that sampling of the singlet probability at one moment in time is often misleading the optimization in weak magnetic field insofar as the increased or decreased probability at the chosen time does not necessarily correlate with an increased or decreased reaction yield. On the other hand, as we have shown, sparse sampling at a moderate sampling density reduces the computational cost while yielding close-to-optimal optimization outcomes and a smooth progression for $B > 1$. We have further demonstrated the applicability of the approach as implemented here to realistically complex radical-pair systems, such as the widely studied Py-DCB exciplex system subject to symmetric recombination. Our suggested approach can serve as a blueprint for future developments and optimizations. Although not explored here, further algorithmic modification could be attempted, such as bottom-up strategies, for which the sampling density is increased as the optimization progresses. Additionally, the optimization blocks could be overlapped. While here these approaches have appeared unnecessary insofar as the suggested approach has yielded control parameters that upon complete optimization did not change significantly subject to the utilized termination criteria of the optimizer, these approaches could further speed up the rate at which this state is reached. Additional computational efficiency could, furthermore, be realized by reformulating the singlet yield evaluation in terms of

the propagation of wave packets, in particular in combination with using an incomplete basis for the nuclear spin functions and trace sampling [68]. We are currently developing such approaches with the aim of extending control to the complete open-systems [69] description of radical-pair systems, including via the incorporation of direct control of the dissipation processes through incoherent control.

As for the calculation of propagators and derivatives, higher-order operator-splitting approaches could be used and the order of the approach, i.e., the accuracy, to the optimization process increased as the target function converges, as has been successfully demonstrated in Ref. [59] for a state-transfer problem. Here, we have again refrained from such additional optimizations, as the generation of propagators and derivatives has not been identified as the most time-consuming step for the considered problem sizes, which is related to the evaluation of reaction yields and gradients instead. From the reaction-control point of view, it is noteworthy that control has allowed us to suppress the singlet recombination to levels below those achievable by application of static magnetic fields of any strength. The achievable recombination yields are, furthermore, well below the recombination yield of 25% expected to ensue for complete randomization of the spin states. This shows that the control fields here do not merely enhance spin relaxation, as one might expect, but drive the system to optimal reaction outcomes.

Finally, we comment on the alternative approach of time-local optimization as introduced in Ref. [8]. Even with the described optimization tweaks, the presented GRAPE-based approach to radical-pair reaction control remains computationally more demanding than the time-local approach. However, it captures the time-integrated nature of the reaction yield, the observable quantity, rather than merely the singlet probability at one moment in time, which is not necessarily a well-defined proxy of the overall recombination yield. Another limitation of the time-local approach is conceptual and is related to the property of permitting only controls that, at every moment of time, increase the optimization target function. This property permits the straightforward derivation of the optimal control amplitudes but constrains the optimizations by excluding controls that would permit a better overall optimization at the cost of a momentary reduction in optimality. We argue that this constraint is critical in the optimization of weak biasing fields. In the Supplemental Material [36], we provide a generalized version of the time-local algorithm from Ref. [8] that permits the optimization of the singlet probability, still for one instance in time, in the presence of spin-selective recombination, as assumed here. Comparing this generalized algorithm to the GRAPE-based approach, we find that it is inferior for optimizing the recombination yield in weak biasing fields, generally requiring larger control amplitudes while still falling short in terms of optimization fidelities.

See the Supplemental Material [36] for the detailed quantitative comparison undertaken for the seven-spin model system. As shown there, superiority of the GRAPE-based approach is realized not only when optimizing the singlet probability at a single time but also when applying a block-wise approach with successively redefined "moving targets." While this time-blocking approach appears auspicious for the time-local approach too, the GRAPE-based approach delivers markedly better yield optimization in weak biasing fields.

The quantum control of radical-pair reactions is still in its infancy. Our present work focuses on the control of the coherent evolution via Zeeman interactions, as this is a modality that is, in principle, addressable with currently available experimental tools without complex changes to the chemistry. We anticipate that optimal control of radical-pair reactions will find applications in the context of biological radical-pair reactions, either as an analytical tool or to drive the systems toward desired outcomes. For example, for biological radical-pair reactions, such as those implicated with magnetoreception, a key problem to be addressed concerns distinguishing between different incarnations of radical reactions to better identify the underlying mechanism in a complex biological environment [65,70,71]. In this scenario, quantum control could allow us to derive control parameters that suppress magnetic field effects in one mechanism while leaving those of alternative competing models unaltered. Ultimately, controls could allow us to turn MFEs into a tool to potentially control reaction processes of physiological relevance for applications in biology and medicine, by facilitating selective stimulation or suppression of cellular functions linked to radical-pair processes. We hope that this work, by building on established techniques from quantum control such as GRAPE to go beyond existing local optimization methods, will lay the groundwork for realizing this.

V. CONCLUSIONS

We have suggested and implemented a GRAPE-inspired approach to control reaction yields of radical-pair recombination reactions through synchronized application of rf magnetic fields in a direction perpendicular to a static biasing field. We deviate from previous approaches by optimizing reaction yields, i.e., the actual experimental observables, instead of fidelity measures defined at a particular time instant. Computational efficiency has been realized by block optimization, sparse sampling, a split operator approach for calculating propagators, and by utilizing curvature information in the nonlinear optimization problem. The approach thus realized is applicable to radical-pair systems of realistic complexity. We have demonstrated that control permits the reduction of the singlet recombination yield of a singlet-born model system to 10%, a yield unattainable by static magnetic field application alone,

when using moderate control amplitudes and bandwidth (cf. Fig. 6). We hope that our approach helps accelerate the adoption of control approaches for radical-pair recombination reactions in low external fields. We anticipate that these future applications will utilize control beyond mere reaction control, e.g., to realize distinguishability of radical pairs in complex environments, and for facilitating model selection for competing hypotheses based on experiments with optimized contrast power.

APPENDIX

1. Sparse blocking

The control of reaction yields via numerical approaches such as GRAPE is expected to be costly. The computational demand is particularly large if, as we do here (and unlike Refs. [8,24]), the goal is to optimize recombination yields of radical-pair reactions, which are time-integral quantities [cf. Eq. (7)]; unlike the typical fidelity measures in quantum control applications pertaining to the implementation of a state transfer or a unitary operation for a fixed time t). The approach requires repeated matrix multiplications for evaluating the time-dependent singlet-probabilities that sum to the recombination yield (and its associated gradients). Formally, Eq. (26) implies

$$\sum_{n=1}^{N}[(n-1)+3]+nL[(n-1)+3]=O(N^3) \quad \text{(A1)}$$

matrix multiplications (i.e., for every t_n, $(n-1)$ matrix multiplications are required to evaluate $\hat{U}$, $(n-1)$ to evaluate $\hat{U}_+\hat{W}_{n,l}\hat{U}_-$ (via $L_{n,l}$) for every l and n; and an additional three each to evaluate the expectation value or the gradients). In practical implementations, the estimate in Eq. (A1) can be improved upon by preserving terms from previous n, i.e., $n-1$. allowing the update of $\hat{U}$ and $\hat{U}_+\hat{W}_{n,l}\hat{U}_-$ with a singular matrix multiplication (instead of $n-1$), thus requiring

$$\sum_{n=1}^{N}4(1+nL)=2LN^2+2(L+2)N \quad \text{(A2)}$$

matrix multiplications. Nevertheless, due to the quadratic scaling of the evaluation of Eq. (27) with N, the gradient

or expectation-value evaluation will often exceed the cost of evaluating the elementary propagators and their derivatives (scaling as N) for large N and thus be the limiting factor. To efficiently optimize the reaction yield of complex radical pairs, we suggest the following adaptation of the gradient-based optimization procedure. We posit that the optimization can be realized in terms of B disjoint blocks of N/B time steps each (time blocking), with the initial state taken as that of the system subject to the preceding optimized controls, sparsely sampled using $N/(BS)$ samples per block, as illustrated in Fig. 3. Here, B and S are integers that divide N and B, respectively. The number of matrix multiplications in this approach is reduced to

$$
B \left(\sum_{n=1}^{N/B} (1 + nL)[1 + 3(\delta_{n \bmod s, 0})] \right)
$$

$$
= B \left(\sum_{n=1}^{N/B} (1 + nL) + 3 \sum_{m=1}^{N/BS} (1 + LS) \right)
$$

$$
= \frac{N^2 L(S + 3)}{2BS} + N \left(2L + 1 + \frac{3}{S} \right). \quad \text{(A3)}
$$

The number of matrix multiplications necessary in general still scales quadratically with N, i.e., as $O(N^2/B)$. Linear scaling is only obtained in the limit that $B = N$, i.e., time-local optimization. But, in practice, the block size can be chosen to be much smaller than N, i.e., $N/B \ll N$, to realize a substantial speedup, while delivering adequate practical optimization of the reaction yield. Furthermore, for $S \gg 3$, the complexity of the algorithm approaches independence of S.

2. Trotter-Suzuki splitting

To efficiently calculate the propagators and the associates Fréchet derivatives, we use a scaling and squaring approach in combination with a Trotter-Suzuki splitting of the elementary propagator. Specifically, we compute the matrix exponent

$$
e^X = \left(e^{2^{-s} X} \right)^{2^s} \quad \text{(A4)}
$$

by $s \in \mathbb{N}$ repeated squaring starting from $e^{2^{-s} X}$, calculated as

$$
e^{2^{-s} X} = e^{-i 2^{-s-1} \Delta t \hat{A}'} e^{-i 2^{-s} \Delta t \hat{A}''} e^{-i 2^{-s-1} \Delta t \hat{A}'} + O \left(\frac{\Delta t^2}{2^{2s}} \right),
$$

with

$$
X = -i \hat{A}' \Delta t - i \hat{A}'' \Delta t \quad \text{(A5)}
$$

being a convenient splitting of $X = -i \Delta t \hat{A}_i$ [cf. Eq. (19)]. In practice, $\hat{A}'$ and $\hat{A}''$ represent the drift and control Hamiltonians, respectively. If the latter is based on coupling

applied magnetic fields via the Zeeman interaction, the propagator under $\hat{A}''$ can be expressed as a direct product of evolution operators for the individual electron spins, based on the expression

$$
e^{-i \omega \hat{n} \cdot S} = \cos \left(\frac{\omega}{2} \right) I - 2i \sin \left(\frac{\omega}{2} \right) \hat{n} \cdot S, \quad \text{(A6)}
$$

where $\omega \in \mathbb{N}$ is a parameter related to the strength of the control field and n in a unit vector specifying the orientation of the perturbation in the laboratory frame.

Likewise, the Fréchet derivative of the exponential e^X can be evaluated using an s-fold recurrence, based on Ref. [72]:

$$
L(X, E) = e^{X/2} L(X/2, E/2) + L(X/2, E/2) e^{X/2}, \quad \text{(A7)}
$$

obtained by differentiating $e^X = (e^{X/2})^2$ using the chain rule. In combination with Eq. (A4), the only derivatives that are explicitly required in this process are those of $e^{-i 2^{-s} \Delta t \hat{A}''}$. For Zeeman coupling with a single spin propagator, as given by Eq. (A6), the necessary Fréchet derivatives can be obtained in analytic form, in combination with the chain rule, from

$$
L(\omega \hat{n} \cdot S, -i \hat{n} \cdot S) = -i \cos \left(\frac{\omega}{2} \right) \hat{n} \cdot S - \frac{1}{2} \sin \left(\frac{\omega}{2} \right) \mathbb{1}. \quad \text{(A8)}
$$

We have optimized using the limited-memory variant of the Broyden-Fletcher-Goldfarb-Shanno (L-BFGS-B) algorithm, that preconditions gradients using curvature information, and used the SciPy [73] implementation with a stopping criterion of 10^{-6} and 10^{-7} for the change of the sparsely sampled yield and the projected gradient, respectively. The maximum number of iterations has been set to 200. Furthermore, we have run simulations in parallel for varying number of blocks B and the sampling interval S, as seen in Figs. 5(a) and 5(b), to assess the performance and scalability of our approach.

---

[1] C. P. Koch, U. Boscain, T. Calarco, G. Dirr, S. Filipp, S. J. Glaser, R. Kosloff, S. Montangero, T. Schulte-Herbrüggen, D. Sugny, and F. K. Wilhelm, Quantum optimal control in quantum technologies: Strategic report on current status, visions and goals for research in Europe, EPJ Quantum Tech. **9**, 19 (2022).

[2] D. J. Tannor, R. Kosloff, and S. A. Rice, Coherent pulse sequence induced control of selectivity of reactions: Exact quantum mechanical calculations, J. Chem. Phys. **85**, 5805 (1986).

[3] D. J. Tannor and S. A. Rice, Control of selectivity of chemical reaction via control of wave packet evolution, J. Chem. Phys. **83**, 5013 (1985).

[4] T. Brixner and G. Gerber, Quantum control of gas-phase and liquid-phase femtochemistry, ChemPhysChem **4**, 418 (2003).

[5] J. P. Dowling and G. J. Milburn, Quantum technology: The second quantum revolution, Philos. Trans. Royal Soc. A **361**, 1655 (2003).

[6] G. G. Guerreschi, M. Tiersch, U. E. Steiner, and H. J. Briegel, Optical switching of radical pair conformation enhances magnetic sensitivity, Chem. Phys. Lett. **572**, 106 (2013).

[7] K. M. Vitalis and I. K. Kominis, Quantum-limited biochemical magnetometers designed using the Fisher information and quantum reaction control, Phys. Rev. A **95**, 032129 (2017).

[8] K. Masuzawa, M. Sato, M. Sugawara, and K. Maeda, Quantum control of radical pair reactions by local optimization theory, J. Chem. Phys. **152**, 014301 (2020).

[9] D. Mims, J. Herpich, N. N. Lukzen, U. E. Steiner, and C. Lambert, Readout of spin quantum beats in a charge-separated radical pair by pump-push spectroscopy, Science **374**, 1470 (2021).

[10] B. Pophof, B. Henschenmacher, D. R. Kattnig, J. Kuhne, A. Vian, and G. Ziegelberger, Biological effects of electric, magnetic, and electromagnetic fields from 0 to 100 MHz on fauna and flora: Workshop report, Health Phys. **124**, 39 (2023).

[11] B. Pophof, B. Henschenmacher, D. R. Kattnig, J. Kuhne, A. Vian, and G. Ziegelberger, Biological effects of radiofrequency electromagnetic fields above 100 MHz on fauna and flora: Workshop report, Health Phys. **124**, 31 (2023).

[12] M. R. Wasielewski, C. H. Bock, M. K. Bowman, and J. R. Norris, Controlling the duration of photosynthetic charge separation with microwave radiation, Nature **303**, 520 (1983).

[13] K. B. Henbest, P. Kukura, C. T. Rodgers, P. J. Hore, and C. R. Timmel, Radio frequency magnetic field effects on a radical recombination reaction: A diagnostic test for the radical pair mechanism, J. Amer. Chem. Soc. **126**, 8102 (2004), pMID: 15225036.

[14] C. T. Rodgers, C. J. Wedge, S. A. Norman, P. Kukura, K. Nelson, N. Baker, K. Maeda, K. B. Henbest, P. J. Hore, and C. R. Timmel, Radiofrequency polarization effects in zero-field electron paramagnetic resonance, Phys. Chem. Chem. Phys. **11**, 6569 (2009).

[15] C. Wedge, C. Rodgers, S. Norman, N. Baker, K. Maeda, K. Henbest, C. Timmel, and P. Hore, Radiofrequency polarization effects in low-field electron paramagnetic resonance, Phys. Chem. Chem. Phys. **11**, 6573 (2009).

[16] G. Grampp, M. Justinek, and S. Landgraf, Magnetic field effects on the pyrene-dicyanobenzene system: Determination of electron self-exchange rates by MARY spectroscopy, Mol. Phys. **100**, 1063 (2002).

[17] T. Mani, Molecular qubits based on photogenerated spin-correlated radical pairs for quantum sensing, Chem. Phys. Rev. **3**, 021301 (2022).

[18] B. K. Rugg, M. D. Krzyaniak, B. T. Phelan, M. A. Ratner, R. M. Young, and M. R. Wasielewski, Photodriven quantum teleportation of an electron spin state in a covalent donor-acceptor-radical system, Nat. Chem. **11**, 981 (2019).

[19] C. J. Wedge, J. C. S. Lau, K.-A. Ferguson, S. A. Norman, P. J. Hore, and C. R. Timmel, Spin-locking in low-frequency reaction yield detected magnetic resonance, Phys. Chem. Chem. Phys. **15**, 16043 (2013).

[20] D. R. Kattnig, F-cluster: Reaction-induced spin correlation in multi-radical systems, J. Chem. Phys. **154**, 204105 (2021).

[21] P. J. Hore and H. Mouritsen, The radical-pair mechanism of magnetoreception., Annu. Rev. Biophys. **45**, 299 (2016).

[22] T. Ritz, R. Wiltschko, P. J. Hore, C. T. Rodgers, K. Stapput, P. Thalau, C. R. Timmel, and W. Wiltschko, Magnetic compass of birds is based on a molecule with optimal directional sensitivity., Biophys. J. **96**, 3451 (2009).

[23] S. Engels, N.-L. Schneider, N. Lefeldt, C. Maira Hein, M. Zapka, A. Michalik, D. Elbers, A. Kittel, P. J. Hore, and H. Mouritsen, Anthropogenic electromagnetic noise disrupts magnetic compass orientation in a migratory bird, Nature **509**, 353 (2014).

[24] A. Tateno, K. Masuzawa, H. Nagashima, and K. Maeda, Anisotropic and coherent control of radical pairs by optimized rf fields, Int. J. Mol. Sci. **24** (2023).

[25] M. Sugawara, General formulation of locally designed coherent control theory for quantum system, J. Chem. Phys. **118**, 6784 (2003).

[26] N. Khaneja, T. Reiss, C. Kehlet, T. Schulte-Herbrüggen, and S. J. Glaser, Optimal control of coupled spin dynamics: design of NMR pulse sequences by gradient ascent algorithms, J. Magn. Reson. **172**, 296 (2005).

[27] R. Geng, T. T. Daugherty, K. Do, H. M. Luong, and T. D. Nguyen, A review on organic spintronic materials and devices: I. Magnetic field effect on organic light emitting diodes, J. Sci. Adv. Mater. Devices **1**, 128 (2016).

[28] H. Lee, N. Yang, and A. E. Cohen, Mapping nanomagnetic fields using a radical pair reaction, Nano Lett. **11**, 5367 (2011).

[29] S. Engmann, E. G. Bittle, and D. J. Gundlach, Magnetic field sensor based on a OLED/organic photodetector stack, ACS Appl. Electron. Mater. **5**, 4595 (2023).

[30] H. Zadeh-Haghighi and C. Simon, Magnetic field effects in biology from the perspective of the radical pair mechanism, J. R. Soc. Interface **19**, 20220325 (2022).

[31] P. de Fouquieres, S. Schirmer, S. Glaser, and I. Kuprov, Second order gradient ascent pulse engineering, J. Magn. Res. **212**, 412 (2011).

[32] E. M. Gauger, E. Rieper, J. J. L. Morton, S. C. Benjamin, and V. Vedral, Sustained quantum coherence and entanglement in the avian compass, Phys. Rev. Lett. **106**, 040503 (2011).

[33] H. A. Rabitz, M. M. Hsieh, and C. M. Rosenthal, Quantum optimally controlled transition landscapes, Science **303**, 1998 (2004).

[34] S. Machnes, U. Sander, S. J. Glaser, P. de Fouquières, A. Gruslys, S. Schirmer, and T. Schulte-Herbrüggen, Comparing, optimizing, and benchmarking quantum-control algorithms in a unifying programming framework, Phys. Rev. A **84**, 022305 (2011).

[35] R. M. Wilcox, Exponential operators and parameter differentiation in quantum physics, J. Math. Phys. **8**, 962 (1967).

[36] See the Supplemental Material at http://link.aps.org/supplemental/10.1103/PRXQuantum.5.020303 for additional results showcasing controllability in the geomagnetic field, robustness of derived controls when applied to simulations incorporating noise, and quantitative comparisons to the time-local approach.

[37] M. M. Hertel, V. P. Denysenkov, M. Bennati, and T. F. Prisner, Pulsed 180-GHz EPR/ENDOR/PELDOR spectroscopy, Magn. Res. Chem. **43**, S248 (2005).

[38] D. R. Kattnig, A. Rosspeintner, and G. Grampp, Magnetic field effects on exciplex-forming systems: The effect on the locally excited fluorophore and its dependence on free energy, Phys. Chem. Chem. Phys. **13**, 3446 (2011).

[39] H. M. Hoang, T. B. V. Pham, G. Grampp, and D. R. Kattnig, Exciplexes versus loose ion pairs: How does the driving force impact the initial product ratio of photoinduced charge separation reactions?, J. Phys. Chem. Lett. **5**, 3188 (2014).

[40] H. Hayashi, *Introduction to Dynamic Spin Chemistry: Magnetic Field Effects on Chemical and Biochemical Reactions*, World Scientific Lecture and Course Notes in Chemistry vol. 8 (World Scientific Publishing Company, Singapore, 2004).

[41] C. Atkins, K. Bajpai, J. Rumball, and D. R. Kattnig, On the optimal relative orientation of radicals in the cryptochrome magnetic compass, J. Chem. Phys. **151**, 065103 (2019).

[42] J. Ramsay and D. R. Kattnig, Radical triads, not pairs, may explain effects of hypomagnetic fields on neurogenesis, PLoS Comput. Biol. **18**, 1 (2022).

[43] R. J. Usselman, C. Chavarriaga, P. R. Castello, M. Procopio, T. Ritz, E. A. Dratz, D. J. Singel, and C. F. Martino, The quantum biology of reactive oxygen species partitioning impacts cellular bioenergetics, Sci. Rep. **6** (2016).

[44] A. A. Lee, J. C. S. Lau, H. J. Hogben, T. Biskup, D. R. Kattnig, and P. J. Hore, Alternative radical pairs for cryptochrome-based magnetoreception, J. R. Soc. Interface **11**, 20131063 (2014).

[45] H. J. Hogben, O. Efimova, N. Wagner-Rundell, C. R. Timmel, and P. Hore, Possible involvement of superoxide and dioxygen with cryptochrome in avian magnetoreception: Origin of Zeeman resonances observed by *in vivo* EPR spectroscopy, Chem. Phys. Lett. **480**, 118 (2009).

[46] J. Deviers, F. Cailliez, B. Z. Gutiérrez, D. R. Kattnig, and A. de la Lande, *Ab initio* derivation of flavin hyperfine interactions for the protein magnetosensor cryptochrome, Phys. Chem. Chem. Phys. **24**, 16784 (2022).

[47] C. C. Winterbourn, Biological chemistry of superoxide radicals, ChemTexts **6** (2020).

[48] A. V. V. Huizen, J. M. Morton, L. J. Kinsey, D. G. V. Kannon, M. A. Saad, T. R. Birkholz, J. M. Czajka, J. Cyrus, F. S. Barnes, and W. S. Beane, Weak magnetic fields alter stem cell-mediated growth, Sci. Adv. **5**, eaau7201 (2019).

[49] B. Zhang, L. Wang, A. Zhan, M. Wang, L. Tian, W. Guo, and Y. Pan, Long-term exposure to a hypomagnetic field attenuates adult hippocampal neurogenesis and cognition, Nat. Commun. **12**, 1174 (2021).

[50] B. König, S. Kümmel, E. Svobodová, and R. Cibulka, Flavin photocatalysis, Phys. Sci. Rev. **3**, 20170168 (2018).

[51] C. Xu, X. Yin, Y. Lv, C. Wu, Y. Zhang, and T. Song, A near-null magnetic field affects cryptochrome-related hypocotyl growth and flowering in arabidopsis, Adv. Space Res. **49**, 834 (2012).

[52] N. S. Babcock and D. R. Kattnig, Radical scavenging could answer the challenge posed by electron-electron dipolar interactions in the cryptochrome compass model, JACS Au **1**, 2033 (2021).

[53] C. F. Martino, P. Jimenez, M. Goldfarb, and U. G. Abdulla, Optimization of parameters in coherent spin dynamics of radical pairs in quantum biology, PLoS ONE **18**, 1 (2023).

[54] K. Schulten and P. G. Wolynes, Semiclassical description of electron spin motion in radicals including the effect of electron hopping, J. Chem. Phys. **68**, 3292 (1978).

[55] D. R. Kattnig, I. A. Solov'yov, and P. J. Hore, Electron spin relaxation in cryptochrome-based magnetoreception, Phys. Chem. Chem. Phys. **18**, 12443 (2016).

[56] H. Mao, G. J. Pažěra, R. M. Young, M. D. Krzyaniak, and M. R. Wasielewski, Quantum gate operations on a spectrally addressable photogenerated molecular electron spin-qubit pair, J. Am. Chem. Soc. **145**, 6585 (2023).

[57] J. Xuereb, P. Erker, F. Meier, M. T. Mitchison, and M. Huber, Impact of imperfect timekeeping on quantum control, Phys. Rev. Lett. **131**, 160204 (2023).

[58] T. Brixner and G. Gerber, Adaptive quantum control of femtochemistry, Phys. Scr. **2004**, 101 (2004).

[59] D. L. Goodwin, P. Singh, and M. Foroozandeh, Adaptive optimal control of entangled qubits, Sci. Adv. **8**, eabq4244 (2022).

[60] M. R. Wasielewski, M. D. E. Forbes, N. L. Frank, K. Kowalski, G. D. Scholes, J. Yuen-Zhou, M. A. Baldo, D. E. Freedman, R. H. Goldsmith, T. Goodson, M. L. Kirk, J. K. McCusker, J. P. Ogilvie, D. A. Shultz, S. Stoll, and K. Birgitta Whaley, Exploiting chemistry and molecular systems for quantum information science, Nature Rev. Chem. **4**, 490 (2020).

[61] J. Cai, G. G. Guerreschi, and H. J. Briegel, Quantum control and entanglement in a chemical compass, Phys. Rev. Lett. **104**, 220502 (2010).

[62] J.-Y. Wu, X.-Y. Hu, H.-Y. Zhu, R.-Q. Deng, and Q. Ai, A bionic compass based on multiradicals, J. Phys. Chem. B **126**, 10327 (2022).

[63] Z. Li, H. Yu, T. Shen, Y. Li, and W. Zhang, Bionic magnetic compass algorithm based on radical pair theory, IEEE Sensors J. **22**, 23812 (2022).

[64] C. D. Aiello, M. Hirose, and P. Cappellaro, Composite-pulse magnetometry with a solid-state quantum sensor, Nat. Commun. **4**, 1419 (2013).

[65] A. Finkler and D. Dasari, Quantum sensing and control of spin-state dynamics in the radical-pair mechanism, Phys. Rev. Appl. **15**, 034066 (2021).

[66] L. D. Smith, F. T. Chowdhury, I. Peasgood, N. Dawkins, and D. R. Kattnig, Driven radical motion enhances cryptochrome magnetoreception: Toward live

quantum sensing, J. Phys. Chem. Lett. **13**, 10500 (2022).

[67] R. Winkler, M. Ciria, M. Ahmad, H. Plank, and C. Marcuello, A review of the current state of magnetic force microscopy to unravel the magnetic properties of nanomaterials applied in biological systems and future directions for quantum technologies, Nanomaterials **13** (2023).

[68] T. P. Fay, L. P. Lindoy, and D. E. Manolopoulos, Spin relaxation in radical pairs from the stochastic Schrödinger equation., J. Chem. Phys. **154**, 084121 (2021).

[69] S. Kallush, R. Dann, and R. Kosloff, Controlling the uncontrollable: Quantum control of open-system dynamics, Sci. Adv. **8**, eadd0828 (2022).

[70] H. G. Hiscock, T. W. Hiscock, D. R. Kattnig, T. Scrivener, A. M. Lewis, D. E. Manolopoulos, and P. J. Hore, Navigating at night: Fundamental limits on the sensitivity of radical pair magnetoreception under dim light, Q. Rev. Biophys. **52**, e9 (2019).

[71] Jingjing Xu *et al.*, Magnetic sensitivity of cryptochrome 4 from a migratory songbird, Nature **594**, 535 (2021).

[72] A. H. Al-Mohy and N. J. Higham, Computing the Fréchet derivative of the matrix exponential, with an application to condition number estimation, SIAM J. Matrix Anal. Appl. **30**, 1639 (2009).

[73] Virtanen *et al.*, SciPy 1.0: Fundamental algorithms for scientific computing in PYTHON, Nat. Methods **17**, 261 (2020).